DØ Detector

Ryuji Yamada

Fermi National Accelerator Laboratory
Batavia, Illinois, USA

1. Introduction

Hadron collider physics turned out very fruitful as shown in the recent results given by UA1 and UA2 groups.[1] The Fermilab Tevatron project already has the CDF detector in its construction stage[2].The construction of a second major collider detector, the DØ detector,[3] was approved in 1984, and will be complimentary to the CDF detector.

Presently the DØ project has now over 90 physicists involved from four national laboratories (BNL, Fermilab, LBL, and Saclay) and 10 universities (Brown, Columbia, Florida State, Maryland, Michigan State, Northwestern, Pennsylvania, Rochester, Stonybrook, and V.P.I.).

2. Design Requirements

As the DØ detector will be built several years after the other existing hadron collider detectors, it should be superior in its many design features compared with them. The DØ detector is designed to have better energy resolution for leptons (e, μ, ν) as well as hadrons than other existing collider detectors. Also it will have much more highly segmented calorimeters than others. UA1 and UA2 detectors have already a few years' operational experiences, and their fundings have been incorporated fully into the design of the DØ detector. It was learned from their experiences that the following are necessary features for the hadron collider detector.

1. Excellent energy resolution for leptons and hardons to study W and Z particles, top quarks andd other unknown particles. The resolution should be good for charged particles as well as for neutral particles to study jets.

2. The detector should be highly segmented to distinguish nearby particles.

3. The detector coverage should be as hermetic as possible to determine the energy of missing particles.

4. For the muon detection, the material for the whole detector should be thick enough in all direction to avoid the punch-through effect of hadron particles.

5. The detector material should be radiation resistant to avoid any change in calibration.

3. General Features of DØ Detector

The DØ detector has no central magnetic field, so the volume for the central detector may be reduced. By utilizing uranium, a high density material, the powerful calorimeter is condensed into the core of the detector. These considerations make possible a highly condensed detector with enormously big radiation and absorption length in all directions with reasonable cost. Still it has excellent energy resolution both for electro-magnetic and hadronic particles, and highly divided segmentation both longitudinally and transversely. Thus this will be a second generation detector.

The perspective cutout view of the assembled DØ detector is shown in Fig. 1, and its elevation view is shown in Fig. 2. The overall structure is symmetrical relative to the collision point. The Energy Doubler beam pipe goes through the center of the detector, and the main ring vacuum pipe goes through the upper part of the calorimeters and end iron toroids.

The calorimeters are made of five separate cryogenic systems: one central calorimeter (CC), two end-cap calorimeters (EC), and two end-plug calorimeters (PC). Inside the central calorimeter the central detectors are contained.

The magnetized iron system is composed of three major parts: one central iron toroid (CF) and two end iron toroids (EF). The bottom plate of the central one supports the central and end calorimeters, and each end iron toroid contains one end-plug calorimeter.

As is shown in Fig. 2, the muon chamber planes, made of layers of proportional drift tubes (PDT), are placed in the space between these toroids and calorimeters (CMA and EMA), and over the whole outside surface of the magnetized irons (CMB and EMB). Other muon chamber planes are placed further away from these toroids (CMC and EMC).

The steel base structure, the platform, which is designed to support and transport the whole detector, is used also for supporting numerous electronics racks, signal and power cabling, and utility piping.

The general overall detector parameters are given in Table 1. The total weight of the detector including the platform is 4750 tons, and its overall dimensions are about 19.8 meters wide, 12.6 meters high and 11.6 meters deep. The outside dimensions of the detector up to the outside surfaces of the toroids are 8.5 meters wide, 8.2 meters high and 8.2 meters deep.

The number of towers of the central, the end-cap, and the plug calorimeters are 12,192, 12,192, and 352 respectively, and the total number of channels is 42,560. The number of muon proportional drift tubes is 12,720. These numbers are significantly more than those of existing detectors.

The performance specifications of the DØ detector is given in Table 2. The energy resolutions of the electro-magnetic and the hadronic events are expected to be 12% /√E and 40% /√E respectively, corresponding to 1.2% and 4% at 100 GeV. The position resolution is expected to be 8mm /√E for the electro-magnetic showers. The transverse segmentation is 0.1 in both ϕ and η, and the longitudinal segmentation is 4 both for the electro-magnetic and hadronic events. The momentum resolution for the muon is 20%, mainly determined by the multiple scattering.

The comparison of the hadron collider detectors is shown in Table 3. It represents the design specifications of the DØ detector, which will be completed in 1989, and the present status of other detectors in the spring of 1985. There will be up-dated parameters for the existing detectors in 1989. It is expected the DØ detector will be used before its completion date for high energy physics with some components missing.

It is clear from this table that the DØ detector is a detector with better energy resolution for both the electro-magnetic and hadronic events, with finer transverse and longitudinal segmentation.

4. Central Detectors

The central detectors are physically contained inside the central calorimeter. The central detectors consist of the central section ($|\eta| < 1.2$) and large angle section ($|\eta| < 3.1$). The central section is made of a vertex detector, layers of transition radiation detectors and layers of drift chambers. They are all cylindrically shaped detectors. The large angle section, which is made of the forward and backward part, has the inner layers of drift chambers, two layers of the transition radiation detectors, and the outer layers of drift chambers. They are shown in Fig. 3. Presently more studies are being carried out for an optimum configuration of the central detector system, and a newer and more efficient arrangement will be proposed.

The vertex detector covers the central collision area. This detector will be used to define the vertex point and also will be useful to study decay vertices of long-lived particles. It will be of particular use in tagging charm or bottom quark decays. This will be useful to distinguish some muons coming from K decays. This detector will be made of proportional drift chambers.

The transition radiation detector will be used to separate electrons from hadrons. The stacks of lithium or polypropylene foils produce the transition radiation x-ray photons, and the succeeding Xe-filled proportional wire chamber wil record the ionization clusters from these photons and reject hadrons. We can expect to achieve a rejection ratio of 50 to 1 for hadrons.

The drift chambers placed outside the transition detector will be primarily responsible for measuring tracks in an event. Each cell contains six sense wires and two delay lines at the inner and outer radius, oriented parallel to the wires. Accuracy of measurement by the sense wires is expected to be 200 μm, and waveform digitization of the anode wire signals will allow two-track separation of 5mm. Measurement of the arrival time at both ends of the delay line allows the determination of the longitudinal coordinate of a track to within ±5mm, and gives a true set of space-point track coordinates.

Measurement of specific ionization on the sense wires will be accomplished using waveform digitizations. In this way rejection of overlapped e^+e^- pairs from photon conversion relative to a single $e^{\pm}$ can be made the level of a few percent.

5. Calorimetry

There is a central calorimeter (CC), two end-cap calorimeters (EC) and two plug calorimeters (PC). Their orientation is shown in Fig. 2. The region covered by each calorimeters are as follows:

Central calorimeter	$45° < \theta < 135°$
End-cap calorimeter	$5° < \theta < 45°$, $135° < \theta < 175°$
Plug calorimeter	$1° < \theta < 5°$, $175° < \theta < 179°$

The boundaries between them are well shared by the neighboring calorimeters to avoid gaps.

To simplify the construction and maintenance, all of these calorimeters are designed to be constructed with the same principle, namely liquid argon calorimeter with depleted uranium plates as absorber material. Moreover, an electro-magnetic calorimeter and its corresponding hadronic calorimeter are packaged into the same vessel for simplicity. However, presently a study is being done on a non-cryogenic plug calorimeter with uranium plates to save cost and construction time.

The choice of the liquid argon calorimeter over other methods was made because of the following reasons:

1. The technique of the liquid argon calorimeter is now well established.
2. It is easy to arrange fine projective tower segmentation and several longitudinal segmentations.
3. An electro-magnetic calorimeter and hadronic calorimeter can be put together into one system, thus simplifying construction.
4. The overall structure of the calorimeter can be made compact by using high density material as absorber.
5. No radiation damage is expected.

6. The gain is stable, because it is a unit gain ion chamber.

7. It is easy to calibrate with charge injection.

8. Once well designed and constructed, its operation and maintenance is easy.

The reasons why the depleted uranium was chosen as the absorber are as follows:

1. Excellent energy resolutions can be achieved for both electro-magnetic and hadronic events: 12% $/\sqrt{E}$ and 40% $/\sqrt{E}$ respectively.

2. By utilizing the compensating effect of uranium nuclear reactions, the energy response for an electro-magnetic event can be made equal to that of a hadron event. This is important for the study of jet's total energy. To verify this effect over wide energy range, test beam experiments are now being carried out at Fermi Lab.

3. By using high density material, the overall size of the detector becomes compact, thus reducing the total cost of the detector.

To simplify the construction, a uniform approach to the calorimeters is taken. Although each calorimeter has its own cryostat, one overall cryogenic system controls all of them. The thickness of uranium plates is chosen 2 and 5mm for all of them. The signal collection of all calorimeters is done by the same type electronic circuitry, and their processing will be done similarly by a standardized system.

The cross section of the central calorimeter is shown in Fig. 4. The heat exchanger for liquifying argon is mounted inside the inner vessel. The sensitive elements are divided into the electro-magnetic, the hadronic and the leakage sections. As is shown in the front view, they are rotated successively to avoid straight azimuthal gaps. In the side view, the sensitive elements are shown to be of a tower structure pointing toward the interaction point.

The side view of the end-cap calorimeter is shown in Fig. 5, which contains the electro-magnetic, the fine hadronic I and II, and the coarse hadronic sections. These sensitive elements are also of a tower structure. At present a study is being carried out to redesign the cryostats for both the central and end-cap calorimeters to reduce the gap between them.

6. Muon System

The muon detection system consists of the magnetized iron toroids and the distributed proportional drift tubes (PDT), as shown in Fig. 2. The coverage of muon detection extends down to 11° with respect to beams. The magnetized iron, one-meter thick, is excited to 2 Tesla except at the corners. The total weight of these three toroids is 3420 tons.

Muons are identified by their characteristics of non-interaction through large absorbers, minimum ionization energy, and relatively long life. Their momenta and charges are determined by the deflection angles in the magnetized iron toroids. Momentum resolution $\Delta p_T/p_T$ is 20% up to p_T=200 GeV/c due to multiple scattering, assuming coordinate measurement accuracy of 0.5mm of PDT's.

In order to detect muons correctly, it is imperative to have enough material to reduce the leaking hadronic shower particles. In DØ geometry, the material in the calorimeter has 6.9 absorption lengths at 90°, and gives a μ/π ratio of about 100. With the addition of one meter steel (6.4 absorption lengths), we can have another factor of 300, and the combined μ/π ratio will be about 3×10^4. The total absorption length at 90° is 13.3, and that at 11° is 18. As is shown in Table III, the total absorption length of the DØ detector is much larger than those of other existing detectors, and this should improve the task of identifying and triggering muons.

There will be three PDT planes relative to one out-going muon; the first plane between the calorimeter and the toroid (A-plane: 4 layers): the second plane just outside the toroid (B-plane: 3 layers); and the third plane further downstream with a lever arm (C- planes : 3 layers). All these planes have their successive layers displaced relative to each other to eliminate left and right ambiguity. In each plane, the wire direction of the tube is aligned approximately parallel to the magnetic field direction.

Presently a couple of different PDT designs are being studied, and their corresponding test models are being constructed and tested. The cross section of one type is shown in Fig. 6. The tubes are extruded aluminum tubes 10cm x 6cm in cross section with field shaping electrodes, and are up to 6 meters long. The individual tube can be snapped together to form layers of tubes. Inside each tube two printed circuit boards will be slid in, each of which have saw-toothed patterns as shown in Fig. 7. One board has the pattern of a long one-cycle saw-tooth, and the other has the pattern of a cyclic saw-tooth with 10cm period as shown in Fig. 8 (Vernier pad). From the charge ratios on these patterns the coordinate of the particle along the wire can be determined. With a chamber of this type, we can measure the position of particles with an accuracy of 0.5mm (FWHM) along the length of the tube.[4]

The total counts of PDT's is about 12,700. Each tube readout requires measurement of one time (TVC) and four charge measurements. The front-end electronics for PDT's will be mounted at one end of the tubes, and will be multiplexed to reduce the number of cables going back to the moving counting room.

7. Trigger and Data Acquisition

At the designed luminosity of 10^{30} cm^{-2} sec^{-1}, it is expected the interaction rate is 10^5Hz. With the present design the data logging is about 1 Hz, because average time available to analyze and reject unwanted triggers is about 100ms. Therefore a reduction of 10^5 is needed in the triggering.

The triggering is done in three levels: the level 0,1, and 2 triggers. The level 0 trigger requires a coincidence between the beam-crossing timing signal and a vertex input from the luminosity monitor counters.

The level 1 trigger consists of the calorimeter trigger and the muon trigger as shown in Fig. 8. The calorimeter trigger is derived from fast sums of signals from pre-amplifiers of both electro-magnetic and hadronic towers. The muon trigger selects out events with muon transverse momenta above 5 GeV/c by two-dimensional matrix logic. This muon cut reduces the muon trigger rate to below 1 Hz.

The results of the level 1 calorimeter trigger and muon trigger are inputed into an AND/OR network in which up to 32 combinations of requirements on multiplicity or thresholds can be selected under computer control. If the trigger is acceptable, then digitization starts.

The level 2 trigger consists of about 50 parallel microprocessors, Micro VAX II's, which take the digitized data from level 1 and refine the various energy, cluster and track variables. The microprocessor then analyzes the events, searching for valid correlations involving electron and muon candidates, missing P_T, total E_T, and jet-like clusters. References

1. Papers of UA1 and UA2 Experiments, This Conference.
2. D. Theriot, Collider Detector at Fermilab (CDF), This Conference.
3. Design Report, the DO Experiment at Fermilab Antiproton-Proton Collider, November 1984.
4. C. Brown et al.,"E-740 Proportional Drift Tube Tests", March 1985, TM-1301 Fermilab Internal Report.

Table I Overall Detector Parameters (March 1985)

Total Weight including Platform	4,750 ton	
Central Detectors		
Vertex Detector	$3 \leq r < 10$cm,	$\lvert z \rvert < 40$cm
Transition Radiation Detectors		
Central	$10 \leq r \leq 40$cm,	$\lvert z \rvert < 60$cm
End	$r < 65$cm,	$92 \leq \lvert z \rvert \leq 122$cm
No. of Channel	1,080	
Drift Chamber		
Central	$40 \leq r \leq 70$cm,	$\lvert z \rvert \leq 74$cm
End	$r < 65$cm,	$80 \leq \lvert z \rvert \leq 137$cm
Uranium Liquid Argon Calorimeters		
Total Gross Weight	786 ton	
Total Weight of Uranium	336 ton	
Total No. of Towers	5,312	
Total No. of Channels	42,560	
Central (active)	$75 \leq r \leq 222$cm	$\lvert z \rvert < 113$cm
No. of Towers	1,536	
No. of Channels	13,952	
End Cap (each) (active)	$r \leq 207$cm,	$142 \leq \lvert z \rvert \leq 350$cm
No. of Towers	1,536	
No. of Channels	12,192	
Plug (each) (active)	$r < 65$cm,	$500 \leq \lvert z \rvert \leq 650$cm
No. of Towers	352	
No. of Channels	2,112	
Muon System		
Total Weight of Toroids	3,420 ton	
Central Toroid	$308 < r_{\perp} < 410$cm	$\lvert z \rvert < 425$cm
	1,880 ton	
End Toroid(each)	$86 < r_{\perp} < 410$cm,	$447 < \lvert z \rvert < 599$cm
	770 ton	
Proportional Drift Tubes	12,720	

TABLE II Performance Specifications

Drift Chamber	
Spatial resolution in $r\Delta\phi$	200 μm
Spatial resolution in z	5 mm
Two track resolution	5 mm in $r\Delta\phi$ 5 cm in Δz
2 overlapped track rejection by dE/dx	50:1
Transition Radiation Detection	
e/π discrimination	50:1
Calorimetry	
Energy resolution - electromagnetic	$12\%/\sqrt{E(GeV)}$
hadronic	$40\%/\sqrt{E(GeV)}$
Segmentation -	$0.1(\Delta\phi)\times 0.1(\Delta\eta)$
transverse	4 in EM
longitudinal	4 in hadronic
Position resolution - EM showers	$8\ mm/\sqrt{E(GeV)}$
Muon System	
Momentum resolution in multiple scattering limit	20%
Transverse momentum for sign determination at 3σ	300 GeV/c
Solid Angle Coverage	
Drift chamber system	$\lvert\eta\rvert<3.5$
Transition radiation detectors	$\lvert\eta\rvert<3.1$
Calorimetry	$\lvert\eta\rvert<4.7$
Muon detection	$\lvert\eta\rvert<2.34$
	$(\Delta\Omega = 98\%)$

Table III Comparison of Hadron Collider Detectors (March 1985)

	DO	CDF	UA1
EM $\Delta E/E$	$.12/\sqrt{E}$	$.14/\sqrt{E}$	$.16/\sqrt{E}$
EM #Towers $90^\circ \pm 45^\circ$	1536	480	26
EM #Samples	4	1	4
Calibration Uncertainty.	$\leq .005$	.01-.02	.03
Hadron $\Delta E/E$	$.4/\sqrt{E}$	$.65/\sqrt{E}$	$.8/\sqrt{E}$
Hadron #Towers $90^\circ \pm 45^\circ$	1536	376	120
Hadron #Samples	4	1	2
#Absorption Lengths	6.9	5.6	5.8
Angular Coverage-Calorim.	$1^\circ-179^\circ$	$2^\circ-178^\circ$	$0.2^\circ-179.8^\circ$
Missing P_T Resolution	$.3/\sqrt{\Sigma E_T}$	$.5/\sqrt{\Sigma E_T}$	$.6/\sqrt{\Sigma E_T}$
Central Field	None	Solenoid	Dipole
Electron Identificaton	TRD+fine Segmentation	P/E+ Calorim.	P/E+ Calorim.
Angular Coverage-Muons	$11^\circ-169^\circ$	$5^\circ-125^\circ$	$30^\circ-150^\circ$
#Absorption Lengths $90^\circ\mu$	13	6	8.2-9.4
$15^\circ\mu$	18	12	8.1
Radiation Damage	None	Some	Some

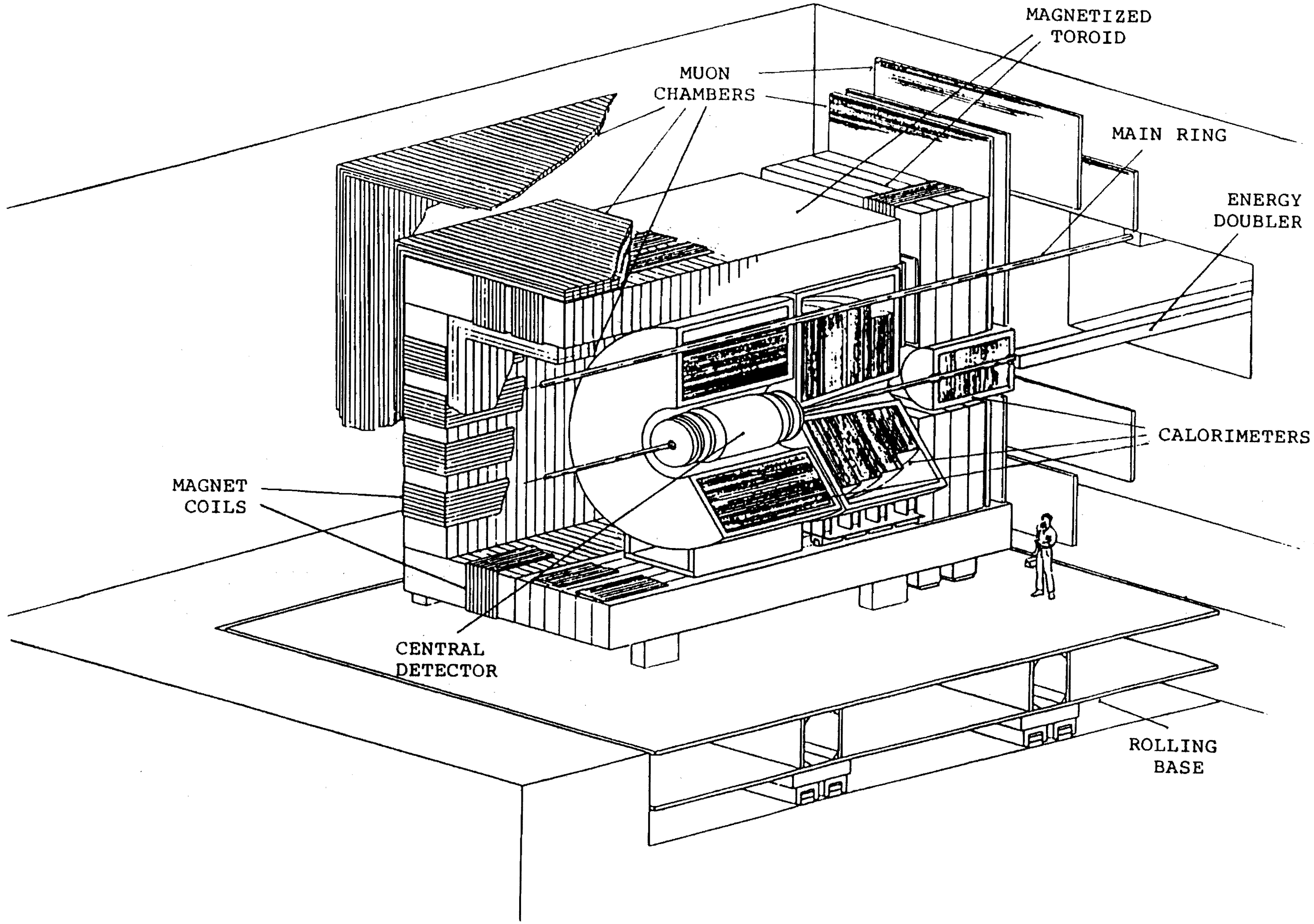

Fig. 1 DØ Detector

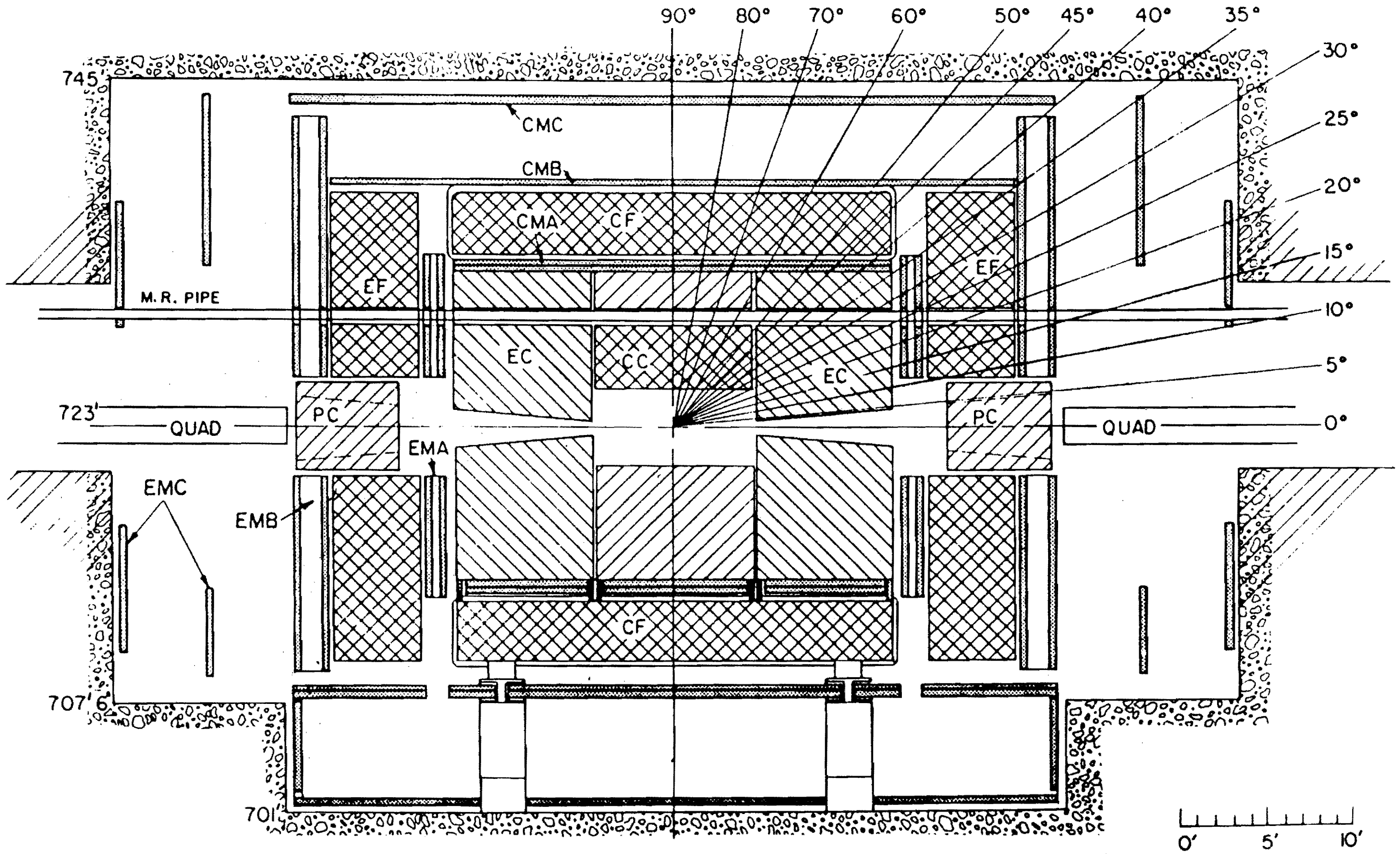

Fig. 2 ELEVATION OF DETECTOR

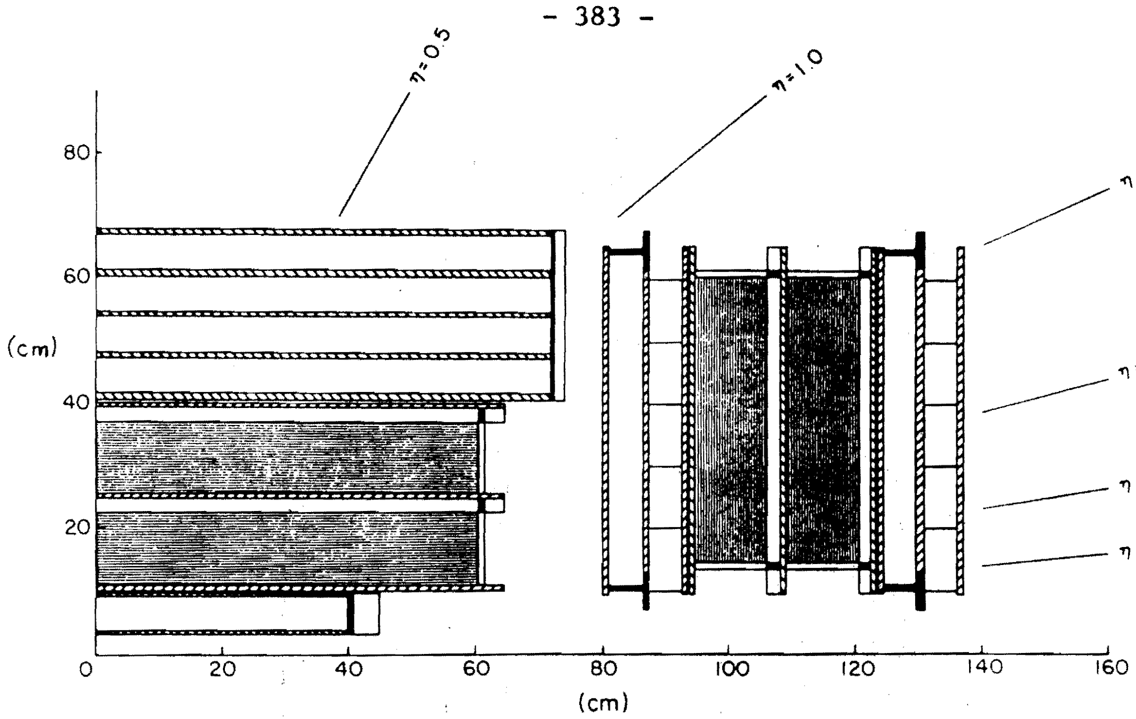

Fig. 3 CENTRAL DETECTOR

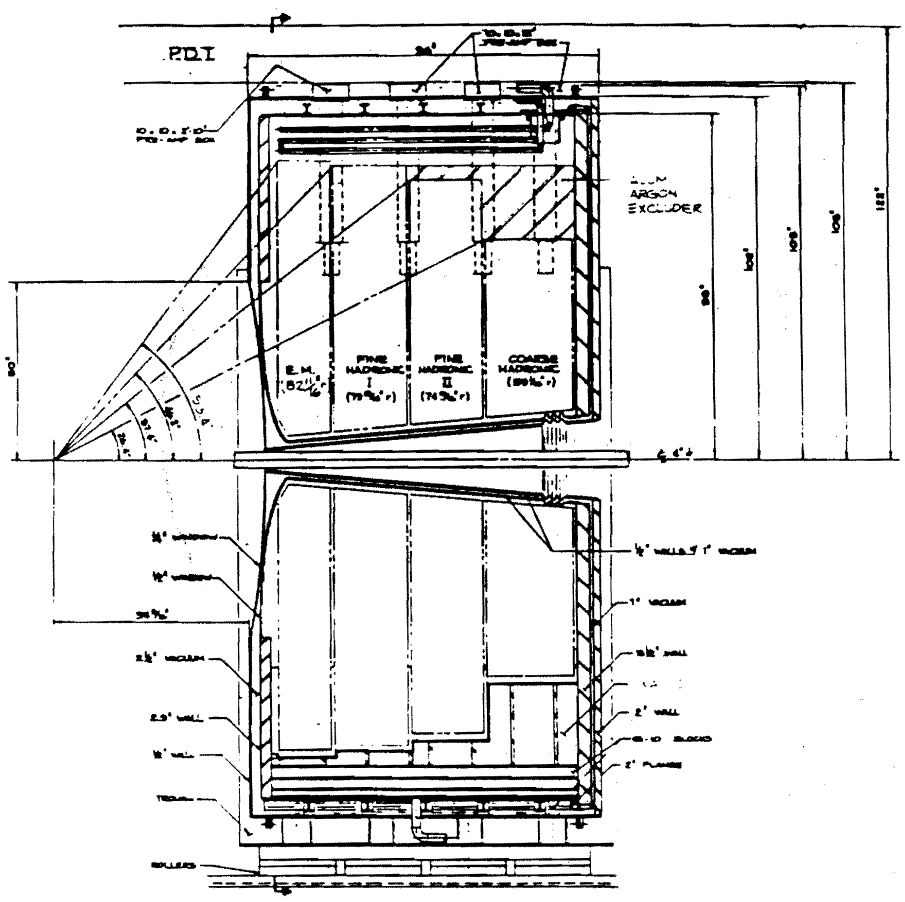

Fig. 5 End Calorimeter

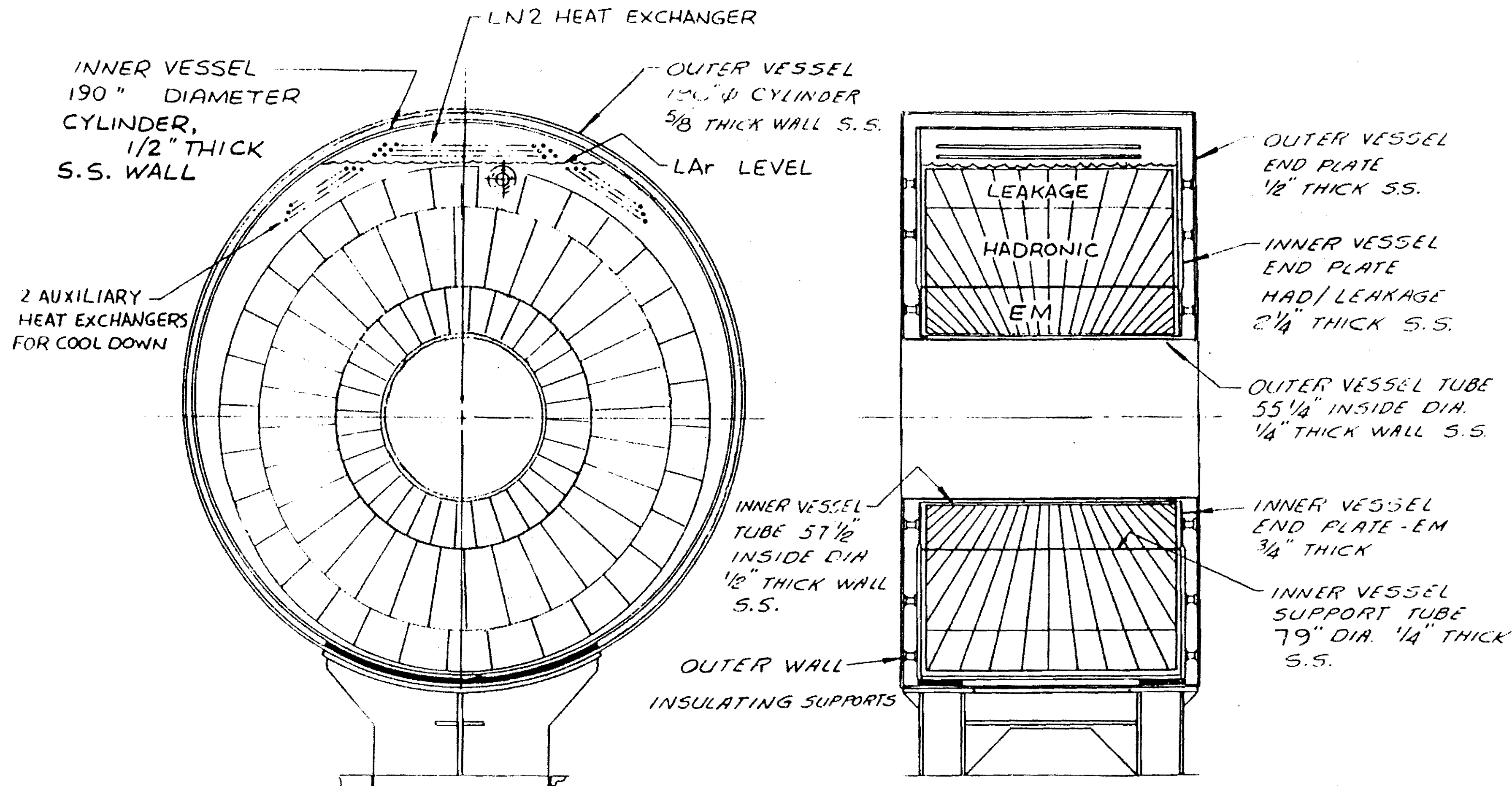

Fig. 4 CENTRAL CALORIMETER
CROSS SECTION

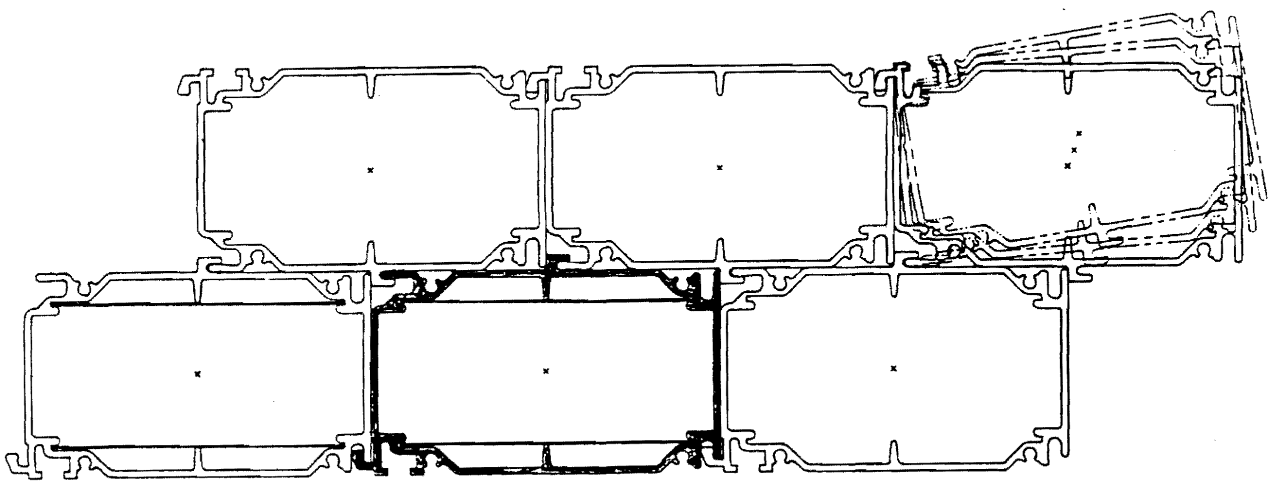

Fig. 6 Cross Section of a Proposed PDT Design

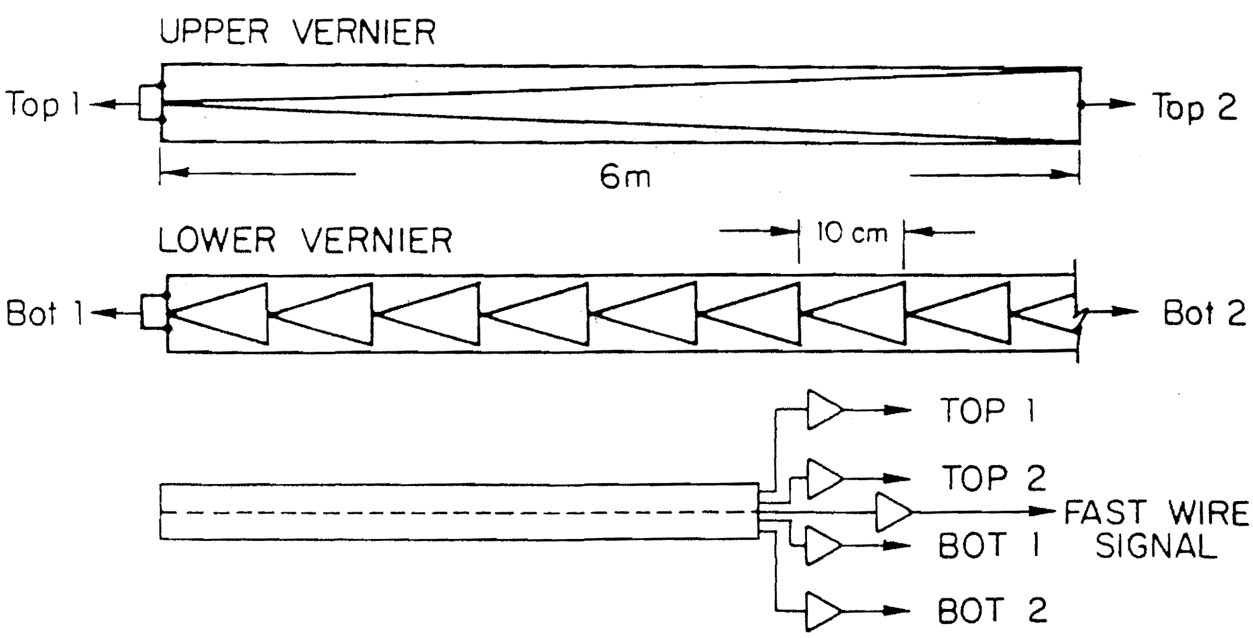

Fig. 7 Pattern for Printed Circuit Board for PDT

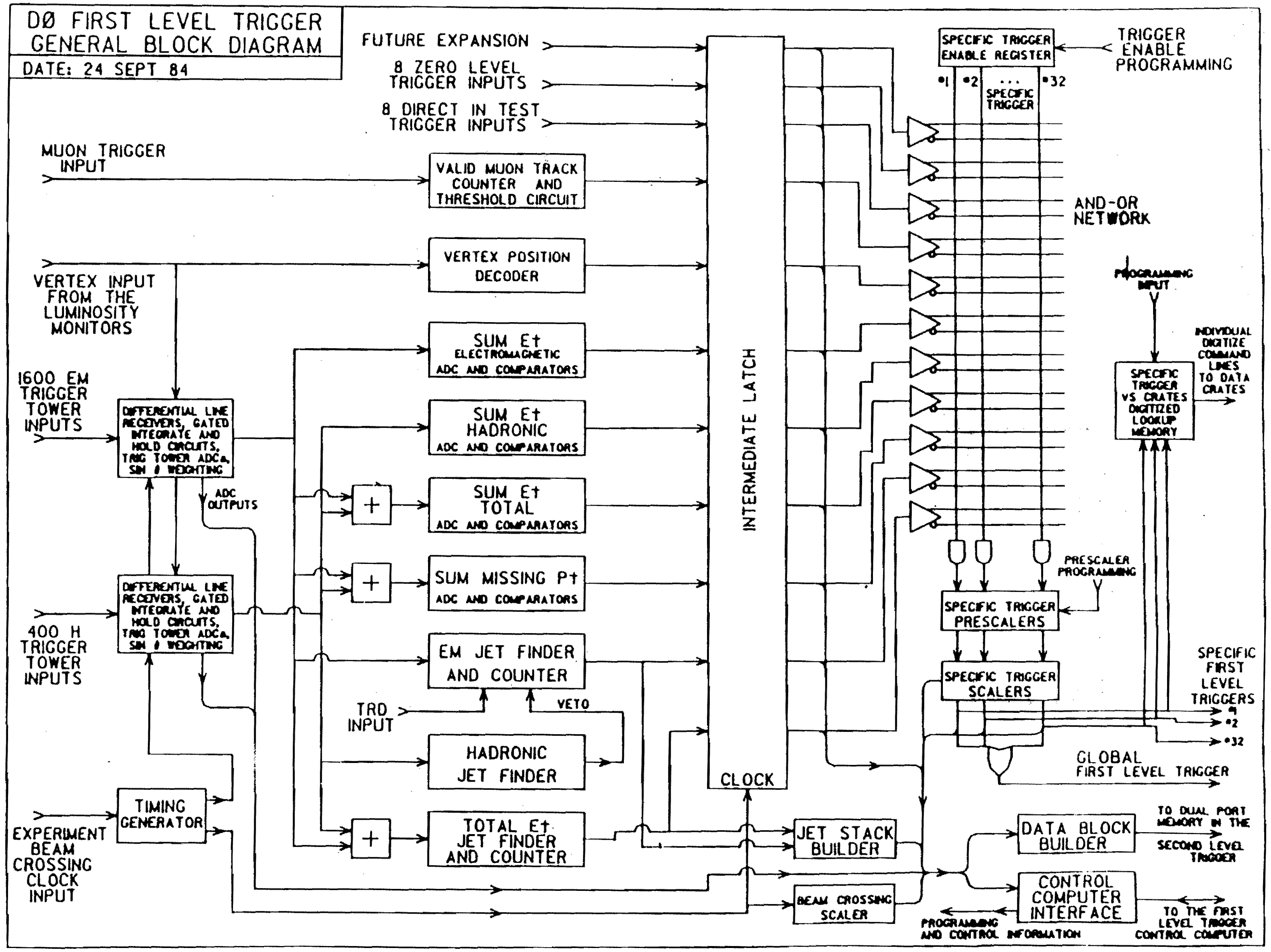

Fig. 8 First Level Trigger